

RAPID COMMUNICATION

Correlated enhancement of H_{c2} and J_c in carbon nanotube doped MgB_2

A Serquis¹, G Serrano¹, S M Moreno¹, L Civale², B Maiorov²,
F Balakirev³ and M Jaime³

¹ Centro Atómico Bariloche—Instituto Balseiro, R8402AGP, S C de Bariloche, Argentina

² Superconductivity Technology Center, MS K763, Los Alamos National Laboratory, Los Alamos, NM 87545, USA

³ NHMFL at Los Alamos National Laboratory, MS E536, Los Alamos, NM 87545, USA

E-mail: aserquis@cab.cnea.gov.ar

Received 22 December 2006, in final form 30 January 2007

Published 26 February 2007

Online at stacks.iop.org/SUST/20/L12

Abstract

The use of MgB_2 in superconducting applications still awaits the development of a MgB_2 -based material where current-carrying performance and critical magnetic field are optimized simultaneously. We achieved this by doping MgB_2 with double-wall carbon nanotubes (DWCNT) as a source of carbon in polycrystalline samples. The optimum nominal DWCNT content for increasing the critical current density, J_c , is in the range 2.5–10 at.% depending on field and temperature. Record values of the upper critical field, $H_{c2}(4\text{ K}) = 41.9\text{ T}$ (with extrapolated $H_{c2}(0) \approx 44.4\text{ T}$), are reached in a bulk sample with 10 at.% DWCNT content. The measured H_{c2} versus T dependences for all samples are successfully described using a theoretical model for a two-gap superconductor in the dirty limit first proposed by Gurevich and co-workers.

The superconductor MgB_2 has great potential for technological applications due to its high critical temperature T_c ($\sim 39\text{ K}$) [1], low cost of raw materials, chemical simplicity and absence of weak-link limitations to the critical current density [2]. In the last few years, several groups have achieved a good improvement of the transport properties of this material, especially in thin films [3–6]. However, in polycrystalline MgB_2 , one of the most important remaining challenges is to increase the upper critical field (H_{c2}), which in the case of undoped clean material is too low for most possible applications [7] while, at the same time, improving the critical current density (J_c). The best results for increasing J_c and the irreversibility field (H_{irr}) in bulk samples are related to an improvement in grain connectivity [5] but also to the addition of suitable defect nanoparticles or doping, i.e. $Mg(B_{1-x}O_x)_2$ [8], SiC [6, 9], Al [10], Dy_2O_3 [11], and carbon nanotubes (CNT) [12–14]. It is well known that pinning of vortex lines to defects in superconductors plays an extremely important role in determining their properties. CNT inclusions, with diameters close to the MgB_2 coherence

length ($\xi_{ab}(0) \sim 3.7\text{--}12\text{ nm}$; $\xi_c(0) \sim 1.6\text{--}3.6\text{ nm}$) [7] may be very good candidates for vortex pinning if they do not completely dissolve in the matrix but remain as tubes acting as columnar defects. In particular, Dou *et al* [12] reported an enhancement of J_c on doping with multi-wall CNT controlling the extent of C substitution during the synthesis (changing the sintering time and temperature) or varying the diameter and length of CNT [13]. However, these studies were made only with samples with a nominal composition $MgB_{1.8}C_{0.2}$.

Another interesting issue is that theoretical models predict that the presence of two superconducting gaps could allow tuning of different upper critical fields by controlling diverse defect sublattices relative to orthogonal hybrid bands [15, 16]. These models predict a significant H_{c2} enhancement in the dirty limit and an anomalous $H_{c2}(T)$ upward curvature. Several reports indicate that H_{c2} can be significantly increased by introducing disorder through oxygen alloying, carbon doping or He-ion irradiation [4, 17–19]. All the record H_{c2} values are reported for films or fibre-textured samples (i.e. Braccini *et al* [4] reported $H_{c2}^{\perp}(4.2) \sim 35\text{ T}$ and

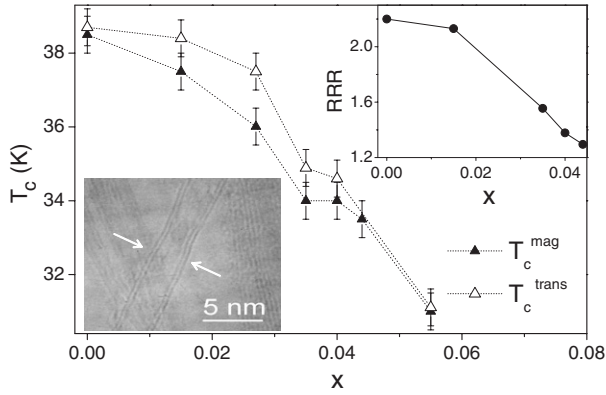


Figure 1. T_c determined from magnetization (solid symbols) and resistivity (open symbols) versus the actual C content (x) as determined by XRD (see the text). The upper inset shows the RRR as a function of x . A typical TEM image of a DWCNT with a 3 nm diameter is displayed in the lower inset (arrows indicate the walls of the DWCNT).

$H_{c2}^{\parallel}(4.2) \sim 51$ T, observed perpendicular and parallel to the ab plane, respectively, in epitaxial MgB_2 C-alloyed films and fibre-textured samples). For carbon doped *bulk* MgB_2 samples much lower extrapolated $H_{c2}(0)$ values of between 29 and 38 T have been reported [20–23].

Although the effect of carbon substitution was one of the most studied in MgB_2 , the results on C solubility and the effect of C doping on the critical temperature (T_c) and critical current density (J_c) reported, so far, vary significantly due to precursor materials, fabrication techniques and processing conditions used, leading to different levels of C substitution and possibly other impurity effects [20–24].

In this work CNT doped MgB_2 samples were prepared by solid-state reaction using as starting materials amorphous boron powder (–325 mesh, 99.99%, Alfa Aesar), magnesium powder (–325 mesh, 99.8%, Assay) and double-walled carbon nanotubes DWCNT (diameter 1.3–5 nm, length ≤ 50 μm , 90%, Aldrich). Details of the reaction procedure will be reported elsewhere [25]. TEM observations were made to characterize the initial composition, main impurities, average CNT sizes, and morphology of the Aldrich DWCNT powder that may affect the pinning properties. The typical DWCNT diameter size of ~ 3 nm (see the lower inset of figure 1) may generate defects to act as effective flux pinning centres. Of the CNT observed, $\sim 90\%$ of these were DWCNT, with the remaining additives being a variety of other kinds of CNT and graphite onion structures, with diameters as large as 15 nm. Amorphous C is also present in the sample and this probably tends to dissolve easily within the MgB_2 structure. The shift in the lattice parameter a , obtained from measured x-ray diffraction patterns, can be used as a measure of the actual amount of C (x) in the $\text{Mg}(\text{B}_{1-x}\text{C}_x)_2$ structure [21]. The x values obtained from using the fitting of the Avdeev *et al* neutron diffraction data [24] and Kazakov *et al* single-crystal data [26] are listed in table 1. It seems that all C is incorporated into the MgB_2 structure for samples with nominal content lower than 5 at.%, while some C does not dissolve for larger nominal contents, indicating that some CNT remain as nanotubes. An increasing

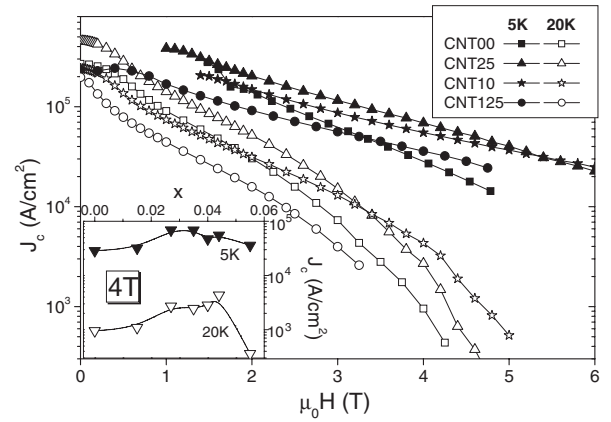


Figure 2. J_c field dependence determined by magnetization for samples CNT00, CNT25, CNT10 and CNT125, at two temperatures 5 K (solid symbols) and 20 K (open symbols). The inset illustrates J_c as a function of x at 4 T and two temperatures, 5 and 20 K.

Table 1. Sample data for nominal DWCNT at.% and actual C content (x). T_c^{mag} and T_c^{trans} were determined from magnetization and transport measurements. The parameters η and g were deduced from the fit of $H_{c2}(T)$ curves with equation (1).

Sample	at.%	x	T_c^{mag}	T_c^{trans}	$\eta = D_{\pi}/D_{\sigma}$	g
CNT00	0	0	38.5	38.7	1	0
CNT01	1	0.015	37.5	38.4	0.1695	0.0018
CNT25	2.5	0.026	36	37.5	0.1288	0.0161
CNT05	5	0.035	34	35	0.1862	0.0291
CNT75	7.5	0.040	34	35.8	0.1409	0.0275
CNT10	10	0.043	33.5	—	0.1212	0.0355
CNT125	12.5	0.052	31	31.1	0.2075	0.0536

broadening of the peaks is observed with increasing C in the samples, which may be related to a larger internal strain [27].

T_c values as determined from magnetization (T_c^{mag}) and resistivity data (T_c^{trans}) are plotted as a function of the actual C content (x) in figure 1. The ΔT_c (90–10%) of the superconducting transitions are lower than 1 K in all cases indicating a homogeneous distribution of the C incorporated into the lattice. The $T_c(x)$ dependence is similar to other reported data [21, 26], but the T_c values are slightly lower for our samples due to an increase in the lattice strain [27]. We observe an increase in the normal state resistivity with x (from 9 to 200 $\mu\Omega$ cm) that is indicative of the shift to a dirty limit. As a consequence, a continuous decrease in the RRR values (defined as the ratio of resistivities $\rho(300\text{ K})/\rho(40\text{ K})$) is observed, as shown in the upper inset of figure 1. If we take into account that values of $\rho \sim 0.4$ – 1.6 $\mu\Omega$ cm were used as typical of MgB_2 films in the clean limit [4], even the $x = 0$ sample (9 $\mu\Omega$ cm) is within the dirty limit. However, there is no simple correlation between the normal state ρ and H_{c2} , because the global resistivity may be limited by poor intergrain connectivity while H_{c2} is controlled by intragrain impurity scattering.

The J_c s and their field dependence calculated from the Bean model [28] are shown in figure 2 for 5 and 20 K. For clarity only a few samples are included. The CNT increase the amount of pinning centres, the optimum doping being temperature and field dependent. This increase may be coming

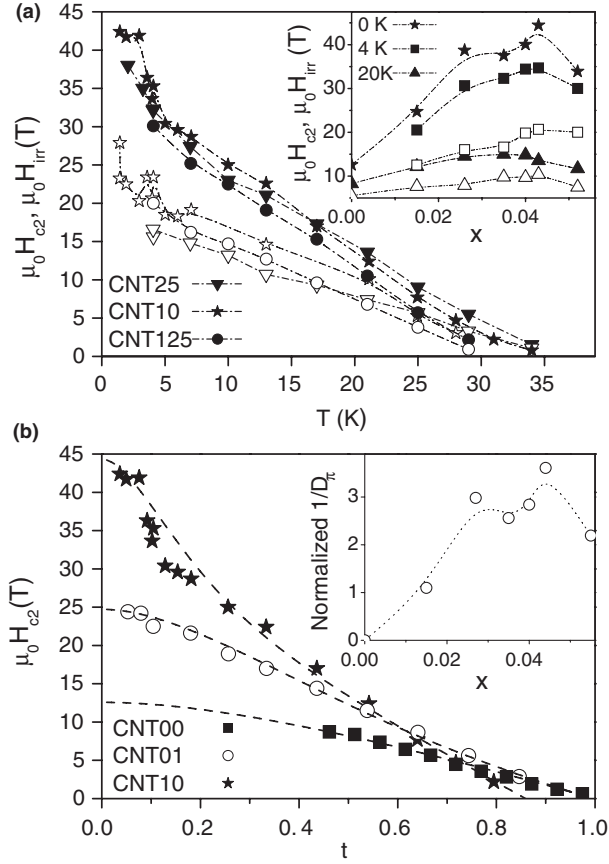


Figure 3. (a) Transport measurements of the upper critical field (H_{c2} , solid symbols) and the beginning of the dissipation (H_{irr} , open symbols) in the $R(H)$ curves for CNT25, CNT10 and CNT125 samples. The inset shows H_{c2} (solid symbols) and H_{irr} (open symbols) as a function of x at 4 K (squares) and 20 K (circles), and the H_{c2} extrapolation at 0 K (stars). (b) H_{c2} versus t for CNT00, CNT01 and CNT10 samples and the fit to data using equation (1) (dashed lines). The inset shows the dependence of $1/D_{\pi}$ with x (the dotted line is a guide to the eye).

in part from pinning of the remaining CNT and in part from C doping. The inset in figure 2 illustrates the J_c performance at 4 T for several samples as a function of x . For nominal contents between 2.5 and 10 at.% we find that J_c is increased up to 5×10^4 A cm $^{-2}$ at 5 T and 5 K. It is apparent that J_c decreases for $x > 0.05$ (nominal content larger than 10 at.%) due to both a larger decrease in T_c and a probable deterioration of interconnectivity between grains denoted by a large ρ (40) value (~ 200 $\mu\Omega$ cm) for the CNT125 sample.

The $H_{c2}(T)$ dependences were determined from four-probe transport measurements in the mid-pulse magnet of NHMFL-LANL, capable of generating an asymmetric field pulse up to 50 T, performed at temperatures between 1.4 and 34 K. Figure 3(a) exhibits the temperature dependences of H_{c2} and H_{irr} , defined as the onset (extrapolation of the maximum slope up to the normal state resistivity) and the beginning of the dissipation, respectively, of the R versus H data for samples with several CNT contents. There is apparent in these $H_{c2}(T)$ data the upward curvature signalled as a characteristic of the presence of two gaps [16, 19]. The inset displays H_{c2} as a function of x for 4 and 20 K and

the extrapolation to 0 K for all samples. We observe that $H_{c2}(0)$ has a maximum near $x \approx 0.045$ for sample CNT10 and a decrease above 0.045 similar to the J_c behaviour. This enhancement is indicating that the incorporation of C in the lattice affects the scattering mechanism, consistent with the RRR variation with x , increasing H_{c2} up to 44 T at 0 K, as predicted by the theoretical models. A lower H_{c2} enhancement is observed in single-wall CNT doped samples [25].

We used equation (1) from [16], obtained from the Usadel equations for a two-gap superconductor in the dirty limit (from Gurevich *et al* [15, 19] and Golubov *et al* [16]) to describe the H_{c2} dependence on temperature observed in CNT doped samples. The proposed model considers that the nonmagnetic impurities affect the intraband electron diffusivities D_{σ} and D_{π} , and the interband scattering rates $\Gamma_{\pi\sigma}$ and $\Gamma_{\sigma\pi}$. We optimized the diffusivity ratio $\eta = D_{\pi}/D_{\sigma}$ and interband scattering parameter $g = (\Gamma_{\sigma\pi} + \Gamma_{\pi\sigma})\nabla/2\pi k_B T_{c0}$, where $T_{c0} = T_c(g = 0)$ to fit the measurements using the following equation [4]:

$$2w(\ln t + U_+)(\ln t + U_-) + (\lambda_0 + \lambda_i)(\ln t + U_+) + (\lambda_0 - \lambda_i)(\ln t + U_-) = 0 \quad (1)$$

where $t = T/T_{c0}$ is the reduced temperature, $U_{\pm} = U_{\pm}(T, H_{c2}, D_{\sigma}, D_{\pi}, \Gamma_{\pi\sigma}, \Gamma_{\sigma\pi})$, $\lambda_i = \lambda_i(\Gamma_{\pi\sigma}, \Gamma_{\sigma\pi})$ and w , λ_0 are constants that depend on λ_{mn} ($m, n = \pi, \sigma$) values obtained from *ab initio* calculations [4, 15, 16].

Figure 3(b) shows $H_{c2}(T)$ as a function of the reduced temperature t , including the experimental values and the curves obtained by fitting the experimental data with the theoretical model of equation (1), for CNT00, CNT01 and CNT10 samples. The upward curvature, characteristic of a two gap effect, is clearly observed near $t \approx 0.2$ for the CNT10 sample. The data for all samples are fitted with the same equation, where a clear difference between them can be explained as an effect of a change in the mechanism of scattering into the bands. This indicates that the two-gap nature is preserved after carbon doping, which is consistent with previous measurements [4, 20]. The fitting parameters η and g are listed in table 1 for all samples. The g values increase with x , as the T_c of the samples decreases. It is worth noting that, although η does not follow a clear tendency, we observe that $1/D_{\pi}$ follows the same dependence of $H_{c2}(0)$ as a function of x (see the inset of figure 3(b)) signifying that C doping is affecting the π -band.

In summary, we prepared samples doped with DWCNT and determined that the actual amount of C in the lattice is less than the nominal CNT content. The decrease in T_c may be explained by assuming not only C incorporation into the lattice but also an increase in the lattice strain. DWCNT doping produced the two desired effects: improvement of J_c and H_{c2} for $0.02 < x < 0.05$. The optimum CNT content for increasing J_c depends on H and T , and it may be further improved by controlling the amount of CNT in the grain boundaries.

$H_{c2}(T)$ can be described using the two-band model [15, 4] for a dirty two-gap superconductor that takes into account the interband scattering. H_{c2} in MgB $_2$ bulk samples may be increased up to record value $H_{c2}(0) \approx 44.4$ T by adding 10 at.% DWCNT. This greatly exceeds the upper critical field performance of other intermetallic superconductors such as Nb $_3$ Sn, confirming that this compound is very attractive for applications.

Acknowledgments

The work at Bariloche was supported in part by CONICET, Fundación Antorchas, and SECYT-PICT. The work at STC-LANL was supported by the Office of Energy Efficiency and Renewable Energy, US Department of Energy. The work at the NHMFL-LANL was supported by the National Science Foundation, the State of Florida and the US Department of Energy. The authors are grateful to Judith L McManus-Driscoll, University of Cambridge, UK, for helpful discussions.

References

- [1] Nagamatsu J, Nakagawa N, Muranaka T, Zenitani Y and Akimitsu J 2001 *Nature* **410** 63–4
- [2] Larbalestier D C *et al* 2001 *Nature* **410** 186–9
- [3] Flükiger R, Suo H L, Musolino N, Beneduce C, Toulemonde P and Lezza P 2003 *Physica C* **385** 286–305 and references therein
- [4] Braccini V *et al* 2005 *Phys. Rev. B* **71** 012504
- [5] Serquis A *et al* 2002 *J. Appl. Phys.* **92** 351–6
- [6] Dou S X, Soltanian S, Horvat J, Wang X L, Munroe P, Zhou S H, Ionescu M, Liu H K and Tomsic M 2002 *Appl. Phys. Lett.* **81** 3419–21
- [7] Buzea C and Yamashita T 2001 *Supercond. Sci. Technol.* **14** R115–46
- [8] Liao X Z, Serquis A, Zhu Y T, Huang J Y, Civale L, Peterson D E, Xu H F and Mueller F M 2003 *J. Appl. Phys.* **93** 6208–15
- [9] Zhou S H, Pan A V, Qin M J, Liu H K and Dou S X 2003 *Physica C* **387** 321–7
- [10] Berenov A, Serquis A, Liao X Z, Zhu Y T, Peterson D E, Bugoslavsky Y, Yates K A, Blamire M G, Cohen L F and MacManus-Driscoll J L 2004 *Supercond. Sci. Technol.* **17** 1093–6
- [11] Chen S K, Wei M and MacManus-Driscoll J L 2006 *Appl. Phys. Lett.* **88** 192512
- [12] Dou S X, Yeoh W K, Horvat J and Ionescu M 2003 *Appl. Phys. Lett.* **83** 4996–8
- [13] Yeoh W K, Horvat J, Dou S X and Munroe P 2005 *IEEE Trans. Appl. Supercond.* **15** 3284–7
- [14] Yeoh W K, Kim J H, Horvat J, Dou S X and Munroe P 2006 *Supercond. Sci. Technol.* **19** L5–8
- [15] Gurevich A 2003 *Phys. Rev. B* **67** 184515–28
- [16] Golubov A A, Kortus J, Dolgov O V, Jepsen O, Kong Y, Andersen O K, Gibson B J, Ahn K and Kremer R K 2002 *J. Phys.: Condens. Matter* **14** 1353–60
- [17] Brinkman A, Golubov A A, Rogalla H, Dolgov O V, Kortus J, Kong Y, Jepsen O and Andersen O K 2002 *Phys. Rev. B* **65** 1805171–4
- [18] Putti M, Braccini V, Ferdeghini C, Pallecchi I, Siri A S, Gatti F, Manfrinetti P and Palenzona A 2004 *Phys. Rev. B* **70** 052509–13
- [19] Gurevich A *et al* 2004 *Supercond. Sci. Technol.* **17** 278–86
- [20] Huang X S, Mickelson W, Regan B C and Zettl A 2005 *Solid State Commun.* **136** 278–82
- [21] Wilke R H T, Bud'ko S L, Canfield P C, Finnemore D K, Suplinskas R J and Hannahs S T 2004 *Phys. Rev. Lett.* **92** 217003–7
- [22] Wilke R H T, Bud'ko S L, Canfield P C, Finnemore D K, Suplinskas R J and Hannahs S T 2005 *Physica C* **424** 1–16
- [23] Senkowicz B J, Giencke J E, Patnaik S, Eom C B, Hellstrom E E and Larbalestier D C 2005 *Appl. Phys. Lett.* **86** 202502–5
- [24] Avdeev M, Jorgensen J D, Ribeiro R A, Bud'ko S L and Canfield P C 2003 *Physica C* **387** 301–6
- [25] Serrano G *et al* 2007 in preparation
- [26] Kazakov S M, Puzniak R, Rogacki K, Mironov A V, Zhigadlo N D, Jun J, Soltmann Ch, Batlogg B and Karpinski J 2005 *Phys. Rev. B* **71** 024533–43
- [27] Serquis A, Zhu Y T, Peterson E J, Coulter J Y, Peterson D E and Mueller F M 2001 *Appl. Phys. Lett.* **79** 4399–401
- [28] Bean C P 1962 *Phys. Rev. Lett.* **8** 250–3